Climate Dynamics (2019) 53:585–600
https://doi.org/10.1007/s00382-018-04603-1

Differential temporal asymmetry among different temperature variables' daily fluctuations

Fenghua Xie[1] · Da Nian[2] · Zuntao Fu[2]

Received: 31 August 2018 / Accepted: 24 December 2018 / Published online: 3 January 2019

Abstract
As one of the most important indicators of nonlinear time series, temporal asymmetric (TA) or temporal irreversible behaviors of daily fluctuations from four temperature variables, including mean temperature (T_{mean}), maximum temperature (T_{max}), minimum temperature (T_{min}) and diurnal temperature range (DTR, $DTR = T_{max} - T_{min}$), have been quantified through both observations and reanalysis over China by two TA measures. One is L_2 from directed horizontal visibility graph and the other is L_1 from consecutive increasing and decreasing steps. The results show that there are differential TA features among daily temperature fluctuations. Firstly, there are marked differences in TA strengths among different temperature variables. It is found that dominated uniformly significant TA (larger than the threshold from corresponding surrogates) emerges in almost all observed T_{mean} fluctuations. However, this kind of uniformly significant TA can't be found in T_{max}, T_{min} and DTR for both observed and reanalysis data sets. Since both TA measures L_1 and L_2 quantify the temporal structures in the given series, this distinguishable TA strengths found in different temperature variables indicates that there are distinct temporal structures in the different temperature variables' variations. Secondly, the TA in each temperature variable is region dependent. The TA strength for each temperature variable is spatially non-uniform with some strong and weak TA regional patterns and these strong and weak TA regional patterns may depend on local weather or climate conditions. Moreover, comparison studies of the same temperature variable reveal that time irreversible features are distinguishable between observations and reanalysis, and this differential feature can be taken as an index to evaluate the quality of reanalysis.

Keywords Daily temperature fluctuations · TA · Differential · Region-dependent

1 Introduction

Asymmetry (spatial or temporal) related studies involve wide fields. Among these asymmetry studies, inter-hemispheric asymmetry in transient global warming (Hutchinson et al. 2013) and asymmetry of ENSO (An and Jin 2004; An 2004; Ye and Hsieh 2006; Douglass 2010; Su et al. 2010; Choi et al. 2012) are two hot topics, especially the warm-cold magnitude asymmetry (An and Jin 2004; Ye and Hsieh 2006; Douglass 2010; Su et al. 2010). At the same time, temporal asymmetry (TA) or time series irreversibility (TI) is ubiquitous in both natural sciences and social sciences (Heinrich 2004; King 1996; Hoyt and Schatten 1998a, b; Livina et al. 2003; Ashkenazy and Tziperman 2004; Lisiecki and Raymo 2005; Bartos and Jánosi 2005; Gyure et al. 2007; Ashkenazy et al. 2008, 2016; Bisgaard and Kulahci 2011; Xie et al. 2016). There are different ordinal patterns dependent on the arrow of time, gradual decreasing-rapid increasing, or quick decreasing-slow increasing (King 1996; Ashkenazy et al. 2008). Therefore, this predominant TA feature can be directly observed in the corresponding time series, since the geometry in the time series is direction-dependent (King 1996). For example, both quarterly numbers of airline passengers and quarterly dollar sales of Marshall Field and Company are decreasing quickly and increasing slowly (Bisgaard and Kulahci 2011). Similar phenomena are more commonly found in various natural science fields. Monthly sunspot records (Hoyt and Schatten 1998a, b; Bisgaard and Kulahci 2011) and seasonal river discharge

✉ Zuntao Fu
fuzt@pku.edu.cn

[1] Department of Atmospheric Science, School of Environmental Studies, China University of Geosciences, Wuhan 430074, China

[2] Lab for Climate and Ocean-Atmosphere Studies, Department of Atmospheric and Oceanic Sciences, School of Physics, Peking University, Beijing 100871, China

(Livina et al. 2003) witness the opposite TA patterns, i.e., increasing rapidly and decreasing gradually. Actually, the signs of TA patterns are closely related to the time scale of corresponding processes. Taking air temperature variations as an example, it is cooling gradually and warming rapidly during the glacial-interglacial cycles (King 1996; Lisiecki and Raymo 2005; Ashkenazy et al. 2008), Heinrich (Heinrich 2004; Ashkenazy et al. 2008) and Dansgaard–Oeschger events (Ashkenazy et al. 2008), and related paleo-climatic changes (King 1996) on long time scales, however, the daily mean temperature variations are rapid cooling and gradual warming at the mid-latitudes (Bartos and Jánosi 2005; Gyure et al. 2007; Ashkenazy et al. 2008).

From these descriptive direction-dependent features, a given process $x(t)$ can be defined as TA or TI if the forward statistical measure from series $\{x_1,\ldots, x_n\}$ is significantly different from the backward statistical measure from the same series (Weiss 1975). The presence of TA features can be taken as a nonlinear indicator for the analyzed time series (Roldan and Parrondo 2010; Lacasa et al. 2012). And this statistical method is also an important indirect way to quantitatively measure the nonlinearity in the analyzed time series (Diks et al. 1995; Stone et al. 1996). Since the TA from the linear processes is distinct from the one from the nonlinear processes, TA has been considered to be an important method for identifying nonlinearity and deterministic chaos in time-series data (Diks et al. 1995; Stone et al. 1996; Li et al. 2015). The method based on TA can distinguish randomness from determinacy in time series, or discriminate chaos from noise (Diks et al. 1995; Stone et al. 1996; Li et al. 2015). This kind of classification is of great importance for understanding the underlying dynamics of analyzed time series, especially for further studies related to nonlinear dynamics, such as climate prediction (Ludescher et al. 2016; Hou et al. 2017; Yuan et al. 2018) (for linear or nonlinear series, different models or methods should be chosen to make prediction) or predictability (Ding et al. 2015, 2016; Li et al. 2018) [previous studies show that increasing nonlinearity may enhance predictability (Ye and Hsieh 2008)]. TA related studies in observational time series have covered various fields such as heart dynamics (Yang et al. 2003; Costa et al. 2005, 2008; Cammarota and Rogora 2006), physiology (Donges et al. 2013), atmospheric sciences (Ashkenazy et al. 2008; Xie et al. 2016; Fu et al. 2016) and ocean dynamics (Ashkenazy et al. 2016).

In order to correctly estimate TA in time series, many statistical methods have been developed (Xie et al. 2016; Lacasa et al. 2012; Cammarota and Rogora 2006; Costa et al. 2008; Donges et al. 2013; Daw et al. 2000). There are both symbolization based (Daw et al. 2000) and symbolization free (Xie et al. 2016; Lacasa et al. 2012) methods. Since the coarse-grained symbolization procedure may bias the TA's quantification (Lacasa et al. 2012), TA measure based on horizontal visibility graph (HVG) (Luque et al. 2009) or visibility graphs (Lacasa et al. 2008) has been developed to exploit the directed link information to quantify TA in any given time series (Lacasa et al. 2012; Donges et al. 2013). Biased TA measure problem can also be solved by considering directly the natural ordinal structures in any given series with its distribution differences of consecutive steps between increasing and decreasing (CSID) (Xie et al. 2016). In this paper, two kinds of symbolization free methods (Xie et al. 2016; Lacasa et al. 2012) will be adopted to calculate the TA measures in four temperature variables' time series.

Since nonlinearity is an intrinsic feature in nearly all the processes in nature, TA or TI should be unveiled from outputs of these processes (Burykin et al. 2011). As mentioned above, air temperature variations (Koscielny-Bunde et al. 1998, 2005; Kiraly and Jánosi 2002; Zhai and Pan 2003; Li et al. 2009; Yuan et al. 2010, 2013; Yuan and Fu 2014) can be taken as the best targeted series to detect TA features. Previous studies found that marked TA feature is hidden in daily mean terrestrial temperature variations (Bartos and Jánosi 2005; Gyure et al. 2007; Ashkenazy et al. 2008; Xie et al. 2016). And this local TA has been confirmed to be directly related to global temporal irreversibility (Xie et al. 2016). Apart from T_{mean}, there are other temperature variables, such as maximum temperature (T_{max}), minimum temperature (T_{min}) and diurnal temperature range (DTR, $DTR = T_{max} - T_{min}$) (Karl et al. 1991, 1993; Weber et al. 1994; Balling et al. 1999; Pattanyus et al. 2004; Lauritsen and Rogers 2012). It has been found there are asymmetric trends in daily T_{max} and T_{min} due to different causal mechanisms in daily T_{max} and T_{min} (Karl et al. 1991, 1993; Weber et al. 1994; Balling et al. 1999; Lauritsen and Rogers 2012). And previous studies have also shown that there are different persistent features in T_{mean}, T_{max}, T_{min} and DTR (Yuan et al. 2010; Pattanyus et al. 2004). Both linear trend and two-point correlation are all linear characteristics of temperature variations. Since there are different linear behaviors among these temperature variations, there may be possibility that they have different conclusions for their nonlinearity. So the first question we want to answer is whether there exists any nonlinear feature difference among T_{mean}, T_{max}, T_{min} and DTR. Specifically, is there a distinguishable time irreversible behavior in the T_{mean}, T_{max}, T_{min} and DTR? Here we need to stress that the general conclusion that the temperature time series is "non-linear" was reported by previous studies mostly for T_{mean} (Bartos and Jánosi 2005; Gyure et al. 2007; Ashkenazy et al. 2008; Xie et al. 2016), little for T_{min}, T_{max} and DTR. At the same time, the "non-linear" temperature conclusion is from different nonlinear measures. We find that conclusion from different nonlinear measures is not consistent. No nonlinear measure can be taken as a sufficient and necessary condition. Studies have shown that two measures from directed HVG (DHVG) and CSID can

lead to consistent results for T_{mean} (Xie et al. 2016). Will there be also consistent results to T_{max}, T_{min} and DTR from two TA measures? Moreover, both the observations (Bartos and Jánosi 2005; Gyure et al. 2007; Xie et al. 2016) and reanalysis (Ashkenazy et al. 2008) data have been used in quantifying TA in T_{mean}, however, no comparison has been carried on the consistence among these results from different data sources. The third problem we want to solve is to assess the quality of different temperature variables' reanalysis data in revealing the TA features. So studies on different temperature variables' series by different nonlinear measures are still an open question. We hope to reach a conclusive answer to these problems in this article.

We arrange the rest of our paper as follows. In Sect. 2, the data source from both observations and reanalysis will be briefly described. Two TA measures from DHVG and CDIS are outlined in Sect. 3. Detailed results will be shown in the Sect. 4, where we will show that there are differential TA behaviors among four temperature variables' fluctuations, two TA measures from both DHVG and CDIS will lead to consistent results, TA behaviors in each temperature variable is region-dependent and there are distinguishable TA behaviors between observed and reanalysis temperature fluctuations. At last, we conclude this paper in Sect. 5 with some discussions.

2 Data

In this paper, both direct observations and National Centers for Environmental Prediction (NCEP) reanalysis (Kanamitsu et al. 2002) for four daily temperature variables (T_{mean}, T_{max}, T_{min} and DTR) were chosen to calculate TA measures.

All observed records for these four temperature variables were downloaded from the China meteorological data sharing service system (http://cdc.cma.gov.cn). There are totally 194 meteorological stations taking part in international exchange. Since there are missing points in some stations, and the data length is too short to reach reliable TA measures for some other stations, records over these stations were not taken into account later. At last, records from 179 stations are selected for further studies, and all records from these 179 stations have been homogenized (Li et al. 2009). The data length over these 179 stations is 57 years, ranging from 1960 to 2016.

The NCEP R-2 (Kanamitsu et al. 2002) not NCEP R-1 (Kalnay et al. 1996) data are used in this paper due to that several human processing errors discovered in NCEP R-1 were fixed and upgraded forecast model and diagnostic package were developed in NCEP R-2 (Kanamitsu et al. 2002). The NCEP reanalysis cover the period from 1979 to 2016, and their horizontal resolutions are $2.5° \times 2.5°$. At the same time, observed temperatures from 1979 to 2016 were also analyzed to compare with the results from NCEP reanalysis. In order to make a direct comparison between the results from direct observations over a specific station and the results from the gridded NCEP reanalysis around this specific station, two-dimensional latitude/longitude gridded meteorological data $f(i,j)$ (where i is latitude and j is longitude) are interpolated to this specific observation station to form the interpolated NCEP station data X_k (k is the station number) by Gaussian weight function (Maddox et al. 1981). The interpolated NCEP station data is given by

$$X_k = \sum_i \sum_j w(i,j) f(i,j) / \sum_i \sum_j w(i,j), \tag{1}$$

where the weight function $w(i,j)$ is

$$w(i,j) = \exp(-d^2(i,j,k)/4C^2). \tag{2}$$

The weight function constant C is chosen to fit data and the distance d is from the grid (i,j) point to the location of the specific station. In this paper, all results from interpolated NCEP station data are from $C = 1.5$. Actually, different choices of the value C make just a little difference for two TA measures (Figures not shown here).

Since in the following TA calculations from both DHVG and CSID only involves temperature variations within 20 days (Xie et al. 2016), and slowly varying periodic variations maybe bias statistical measures of fast fluctuations (Deng et al. 2018), especially for the TA estimation for some TA measures (Ashkenazy et al. 2008), these long time-scale variations (such as seasonal trend) were filtered out by subtracting the annual cycle, $T_i' = T_i - \langle T_i \rangle$ (Koscielny-Bunde et al. 1998), where T_i is any given daily temperature and $\langle T_i \rangle$ is its long-time climatological average for each calendar day. It should be pointed out that such procedure can not eliminate slow linear or nonlinear background trends (Bartos and Janosi 2005; Deng et al. 2018).

In order to reach reliable statistical results, uncertainties of the estimated TA measures must be provided. In this paper, data-driven statistical tests were applied to quantify the uncertainties of estimated TA measures at any given significance level. Therefore, surrogates were generated from the original fast temperature fluctuations T_i' by means of surrogate procedures. Model free surrogate procedures (Schreiber and Schmitz 1996; Eichner et al. 2007; Makse et al. 1996; Govindan et al. 2007) such as Fourier-filtering techniques and shuffling (Makse et al. 1996; Govindan et al. 2007) can be adopted to produce surrogated data of temperature fluctuations T_i'. In this paper, only phase randomize surrogate procedure (PRS) introduced by Schreiber and Schmitz (1996) and Eichner et al. (2007) was carried out in order to preserve the linear features of the original temperature fluctuations T_i' unchanged. The PRS method to generate the surrogates is based the Fourier transform of the analyzed data and then replacing its phase with random numbers, at

last the adjusted Fourier transform of the analyzed data is inversely Fourier transformed to reach a surrogate with the same power spectral density as those of the analyzed data. Since different random numbers can be chosen in the second step of this phase randomize surrogate procedure, we can generate an ensemble of surrogates by this method, too. In this paper, there are 1000 samples for each ensemble. These 1000 samples were used to calculate the critical threshold of two TA measures to distinguish linear series from outputs of nonlinear processes.

3 Methods

3.1 DHVG and CSID

For any given real-value series$\{x_t\}_{t=1,2,\ldots,N}$, where N is its data length, according to DHVG, each point can be taken as a node. Two points x_i and x_j in the series are mapped to links between two nodes i and j in the graph according to DHVG (Lacasa et al. 2012; Luque et al. 2009; Donner et al. 2010):

$$x_n < x_i, x_j,\ \forall\, n | i < n < j, n | i > n > j. \tag{3}$$

A schematic picture of what TA and TI are measuring is shown in Fig. 1. Taking an idealized periodic series, $\{x_{ij}, i=1, 2, 3, \ldots, N;\ j=1, 2, 3, 4, 5\}=(1, 2, 3, 5, 2.5, 1, 2, 3, 5, 2.5, 1, 2, 3, 5, 2.5, \ldots, 1, 2, 3, 5, 2.5)$, as an example to illustrate how DHVG and CSID work for any given series to quantify TA or TI. For simplicity, we only show the results for $N=20$ from this idealized periodic series, more complex series can be similarly analyzed and qualitative features are unchanged. From the plot of this series, we can see that it is asymmetric due to an asymmetric local triangular structure with consecutive increasing three steps (x_{i1}, x_{i2}, x_{i3}) followed by consecutive decreasing two steps (x_{i4}, x_{i5}). According to the DHVG, each point in the series is taken as a node, two points x_i and x_j are linked if for any given point x_n with $i<n<j$ or $i>n>j$, $x_n<x_i$ and $x_n<x_j$. For series given in Fig. 1, taking x_{44} as an example, since x_{11} and x_{22} are smaller than x_{33}, so there only one link between x_{33} and x_{44}, which is taken an ingoing link of node x_{44} for it is from the past of x_{44}; because x_{94} is larger than x_{55}, x_{61}, x_{72}, x_{83}, there is only a link between x_{94} and x_{44}, similarly, there is a link between x_{83} and x_{44}, between x_{55} and x_{44}, and all these three links are from the future of x_{44}, which are defined as outgoing links of node x_{44}. An ingoing link and three outgoing links, which are labeled as (1, 3), are all links for node x_{44}, see Fig. 1a. Similarly all nodes with their ingoing and outgoing links can be labeled as (k_{in}, k_{out}) in each specific node in the plot. Based on the k_{in} and k_{out} for all nodes, the TA/TI measure can be defined and calculated.

Figure 1b shows how the natural local increasing and decreasing trends can map the analyzed series to a persistent

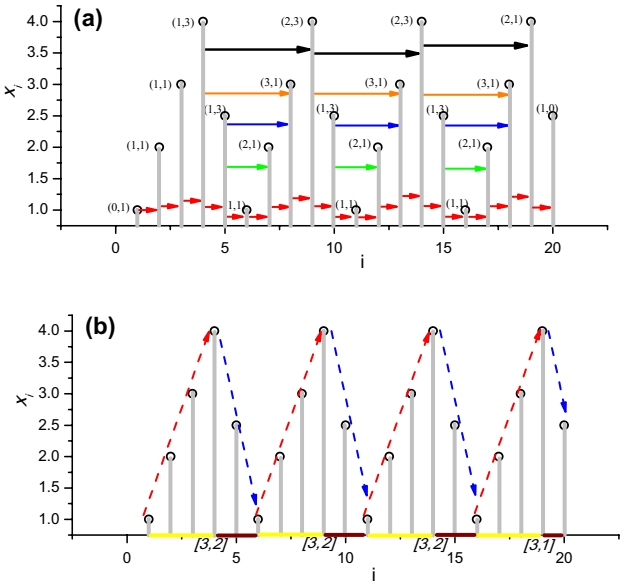

Fig. 1 Schematic picture of DHVG and CSID. **a** DHVG, **b** CSID, where different color horizontal arrows in **a** denote the links between both nodes, red for two close neighbor nodes, green for two nodes separated by other one node, blue for two nodes separated by other two nodes, black for two nodes separated by other three nodes with (k_{in}, k_{out}) for each node; and dash arrows with different colors in **b** denotes natural local trends, red for consecutive increasing trend and blue for consecutive decreasing trend with the horizontal colored lines showing the steps for consecutive increasing or decreasing trend, yellow for increasing and wine for decreasing with $[i, d]$ for each increasing and decreasing trend

trend step length series. Since there is only an asymmetric local triangular structure with consecutive increasing three steps (x_{i1}, x_{i2}, x_{i3}) followed by consecutive decreasing two steps (x_{i4}, x_{i5}), the step length series can be coarsely grained with local pattern $[i, d]=[3, 2]$ or $[3, 1]$. Since only local permutation is taken into account in CSID, the measure from CSID is more robust to noise and low frequency trend, which are common in temperature records (Gao and Franzke 2017). For example, if the above given idealized series are transformed by locally rescaling as (1, 2, 3, 4, 2.5, 0.8, 1.6, 2.4, 3.2, 2, 1.2, 2.4, 3.6, 4.8, 3,…), then the results from CSID are the same due to the unchanged local natural trend, but the results from DHVG are different, since more links from remote nodes available due to the larger magnitudes' variations of some nodes.

So for any given real-value series$\{x_t\}_{t=1,2,\ldots,N}$, the degree $k(t)$ is decomposed into ingoing degree $k_{in}(t)$ and outgoing degree $k_{out}(t)$. Correspondingly, their distributions of the ingoing degree $k_{in}(t)$ and the outgoing degree $k_{out}(t)$ are estimated as $p_{in}(k)$ and $p_{out}(k)$. Similarly, for this series$\{x_t\}_{t=1,2,\ldots,N}$, each data point can be grouped into two states according to its ordinal structure with its neighboring points: decreasing $x_n<x_{n-1}$ and increasing $x_n>x_{n-1}$.

And then according to CSID, distributions of consecutive s increasing or decreasing steps can be estimated as $p_i(s)$ or $p_d(s)$ (Xie et al. 2016).

3.2 Measures for TA or TI

In this paper, measure for TA or TI is defined by the absolute distance between two probability distributions $p(x)$ and $q(x)$ (Xie et al. 2016):

$$L(p,q) = \sum_{x\subset\chi} |p(x)\log p(x) - q(x)\log q(x)|. \tag{4}$$

Combining results from DHVG and CSID with Eq. (4), the distance between $p_d(s)$ and $p_i(s)$ is

$$L_1(p_d,p_i) = \sum_{s} \left|p_d(s)\log p_d(s) - p_i(s)\log p_i(s)\right|, \tag{5}$$

while that between $p_{in}(k)$ and $p_{out}(k)$ is

$$L_2(p_{in},p_{out}) = \sum_{k} \left|p_{in}(k)\log p_{in}(k) - p_{out}(k)\log p_{out}(k)\right|. \tag{6}$$

The measure (4) has been compared with two well defined measures (Xie et al. 2016), the Kullback–Leibler divergence (Cover and Thomas 2006; Kowalski et al. 2011) and Euler distance between two distributions (Cover and Thomas 2006; Kowalski et al. 2011). It was confirmed (Xie et al. 2016) that both the Kullback–Leibler divergence and Euler distance could result in the similar results as the measure (4). For the time series from the real world, the measure (4) works a little better than both the Kullback–Leibler divergence and Euler distance (Xie et al. 2016). So in this paper, all results will be shown based on the measures (5) and (6). Here it should be pointed out that since L_1 from (5) quantifies asymmetry related to the local natural trend, it is more suitable to measure symmetry of gradual cooling and fast warming or fast cooling and gradual warming found in temperature variations. L_1 is only related to the local permutation not magnitude, so it is robust to noise or low-frequency variations. Contrarily, L_2 from (6) may suffer from the effect of the isolated extreme value, which may provide remote links, so L_2 is not so robust to noise or low-frequency variations compared with L_1. And L_2 may provide different information from those given by L_1, such as magnitude variation of isolated extreme value.

4 Results

4.1 Distinct TA strength in different temperature variables

In Fig. 2, we show the spatial distribution of TA measure L_2 from four daily surface temperature variables' (including T_{mean}, T_{max}, T_{min} and DTR) observed records. For comparative purpose, the same color bar is set for each

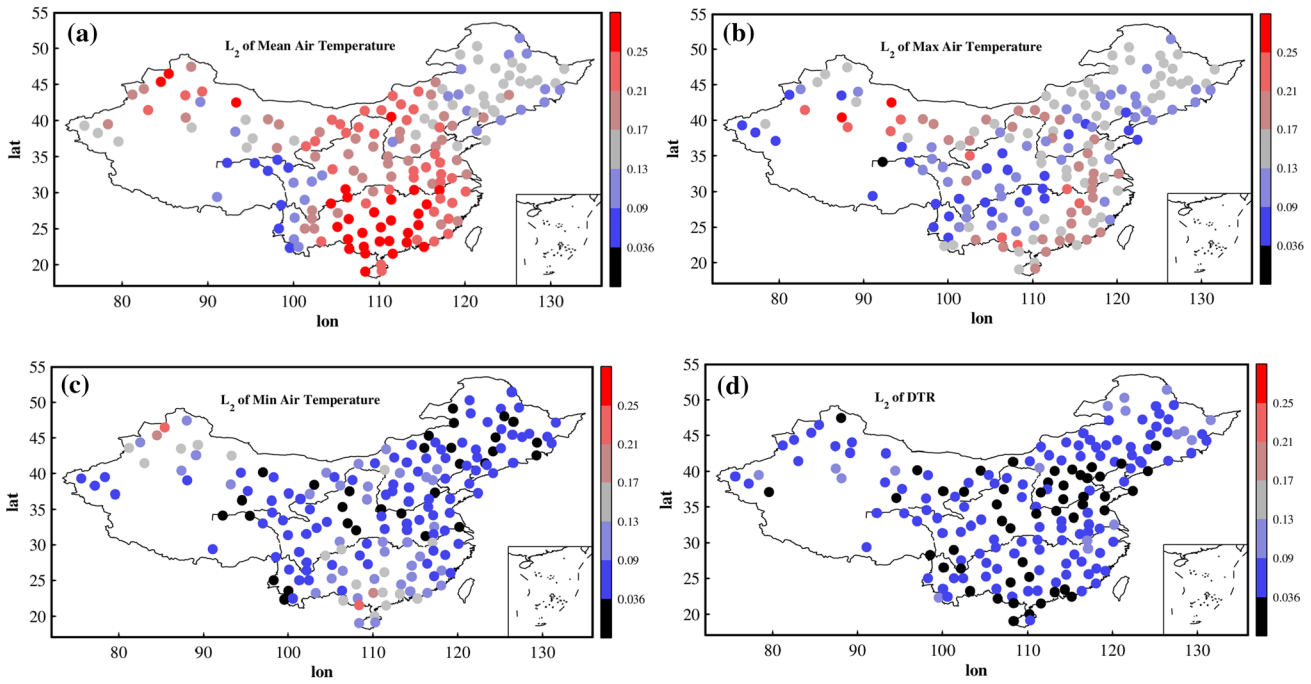

Fig. 2 L_2 to **a** T_{mean}, **b** T_{max}, **c** T_{min}, **d** DTR from 1960 to 2016 for station observations, where 0.036 is critical threshold of L_2 at the significance level of 95% and solid black dots indicate L_2 is below this critical threshold

temperature variable. It is obvious that the TA strength is different among different temperature variables.

Here, in order to check the statistical significance of estimated TA measure L_2, surrogates from PRS procedure (each group has 1000 samples) with the same linear features (such as linear correlation) were carried out the same calculation to obtain 1000 values of TA measure L_2. Among these 1000 values of TA measure L_2, the 950th value (from the minimum to the maximum) was set as a critical threshold L_{2c} (which is corresponding to standard 95% confidence interval). Since all the surrogates have the same data length and linear features as each original temperature variables' fluctuations, this critical threshold L_{2c} can be taken as a benchmark to distinguish the statistically significant L_2 from statistically insignificant L_2 or temporal symmetric L_2. The similar course can be manipulated on estimated TA measure L_1 to derive the critical threshold L_{1c}. It should be noted that the specific value for each critical threshold may change when time series of different data length is taken to calculate the estimated TA measure.

For Figs. 2 and 3, the data length spans from 1960 to 2016, the value of L_{2c} is 0.0360, and L_{1c} is 0.0349. And these critical thresholds were marked as the lowest color level in spatial distributions of estimated TA measure (see the solid black dots in Figs. 2, 3). The same critical thresholds were marked in the scatter plots with dash lines, horizontal or vertical, see Fig. 4. When length span of analyzed temperature fluctuations is changed from 1979 to 2016 (see Figs. 5, 6, 7, 8), the value of L_{2c} is 0.0459, and L_{1c} is 0.0456.

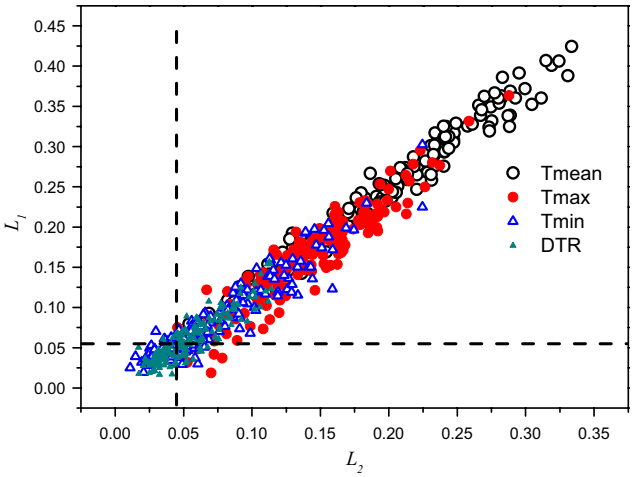

Fig. 4 Scatter plots for L_1 vs. L_2 for T_{mean}, T_{max}, T_{min} and DTR from 1960 to 2016 for station observations. The horizontal and vertical dash black lines denote the critical thresholds of L_1 and L_2 at the significance level of 95%, respectively

When the value of the estimated TA measure, L_2 or L_1, is below the established threshold, the analyzed series is taken to be statistically insignificant TA or temporal symmetric (at confidence level larger than 95%). On the contrary, when the value of the estimated TA measure, L_2 or L_1, is larger than

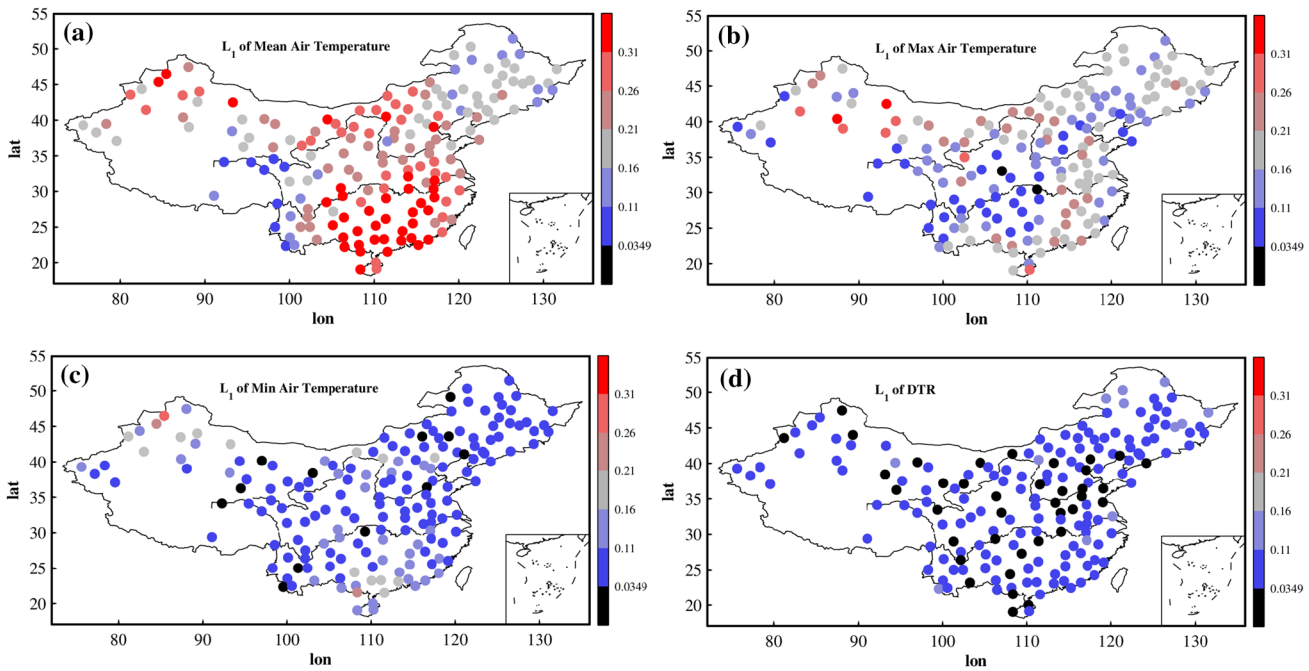

Fig. 3 L_1 to **a** T_{mean}, **b** T_{max}, **c** T_{min}, **d** DTR from 1960 to 2016 for station observations, where 0.0349 is critical threshold of L_1 at the significance level of 95% and solid black dots indicate L_1 is below this critical threshold

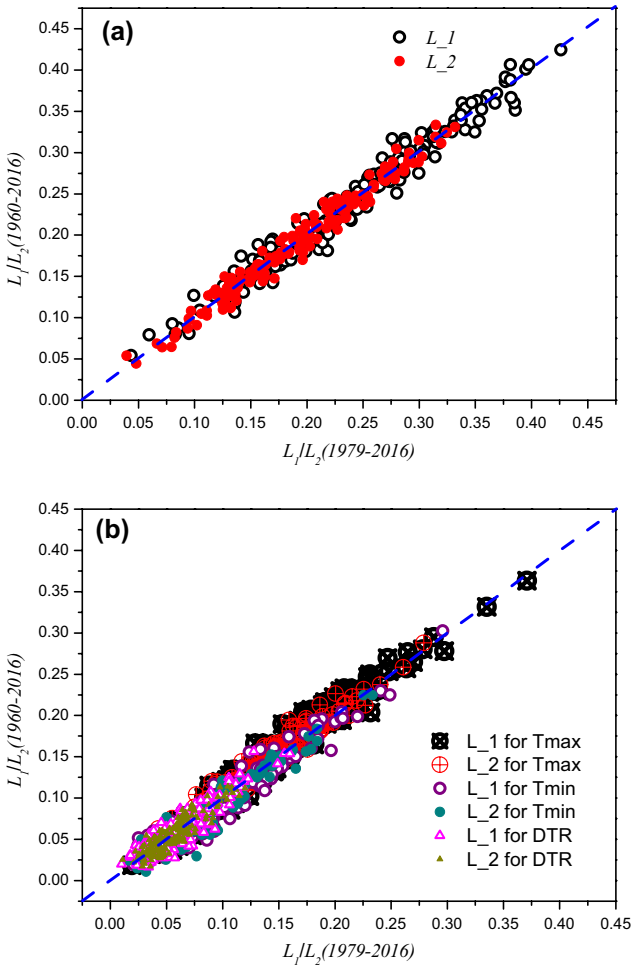

Fig. 5 Scatter plots for station observations, **a** L_1 (L_2) from 1979 to 2016 vs. L_1 (L_2) from 1960 to 2016 for T_{mean}, **b** L_1 (L_2) from 1979 to 2016 vs. L_1 (L_2) from 1960 to 2016 for T_{max}, T_{min} and DTR

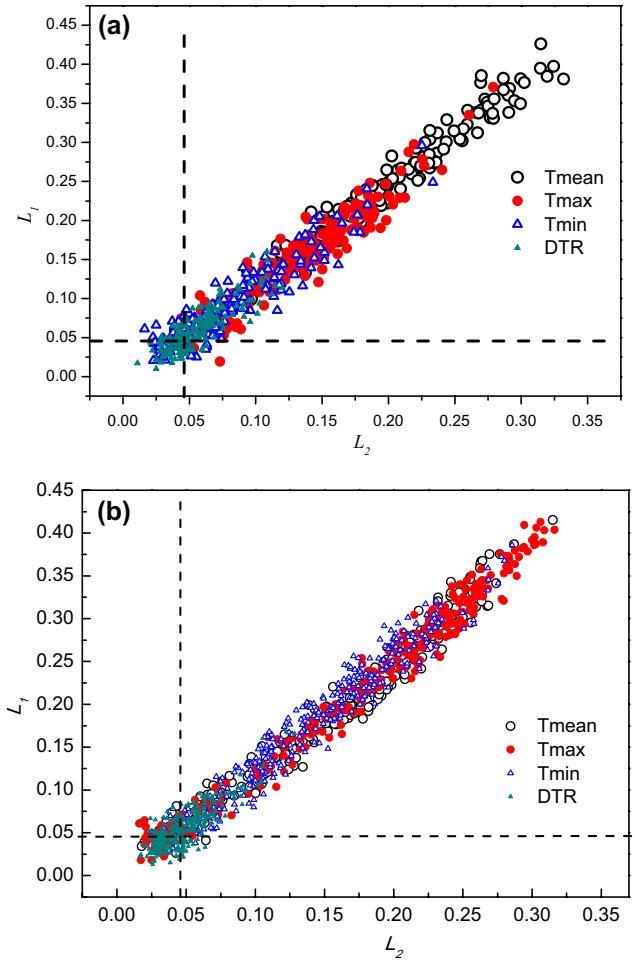

Fig. 6 Scatter plots for **a** L_1 vs. L_2 for T_{mean}, T_{max}, T_{min} and DTR from 1979 to 2016 for station observations, **b** L_1 vs. L_2 for T_{mean}, T_{max}, T_{min} and DTR from 1979 to 2016 for interpolated NCEP station. The horizontal and vertical dash black lines denote the critical thresholds of L_1 and L_2 at the significance level of 95%, respectively

the established threshold, the analyzed series is statistically significant TA (at confidence level larger than 95%).

Obviously, the dominated uniformly significant TA emerges in observed daily T_{mean} fluctuations, see Fig. 2a. All observed daily T_{mean} fluctuations are statistically significant TA (at confidence level larger than 95%). Among them, more than half of the 179 analyzed T_{mean} fluctuations have their estimated L_2 larger than 4 times of L_{2c} (which can be taken as an extreme TA index), with a national scale averaged value of 0.19. The strength of TA in T_{mean} is really high and these results are consistent with previous findings (Xie et al. 2016).

Contrary to more TA studies to daily T_{mean} fluctuations, less study has been devoted to other three temperature variables. Comparing Fig. 2a with Fig. 2b–d, we can learn that the TA strength of other three variables is much weaker than those for T_{mean}. Among them, the TA strength of T_{max} is only weakened a little, see Fig. 2b. The observed daily T_{max} fluctuations over only one station are statistically insignificant TA. There are still more than half of the 179 analyzed T_{max} fluctuations with their estimated L_2 larger than 3 times of L_{2c}, with a national scale averaged value of 0.14. However, the station numbers with extreme TA index are greatly reduced, the TA strength of the T_{max} fluctuations over only 10 stations is larger than 4 times of L_{2c}.

The TA strength of the T_{min} fluctuations is further reduced, see Fig. 2c. Although the value of L_2 over two-thirds of stations is still larger than L_{2c}, there are only 2 stations evidencing their TA strength larger than 4 times of L_{2c}.

Contrary to the marked TA in T_{mean}, TA behavior in DTR is totally different, where TA is much weaker, see Fig. 2d. Nearly one-third of L_2 values in DTR are below the critical value $L_{2c}=0.0360$, and other two-thirds close to the critical value L_{2c} 0.0360. And most of important, no station evidences its TA strength larger than 4 times of L_{2c}.

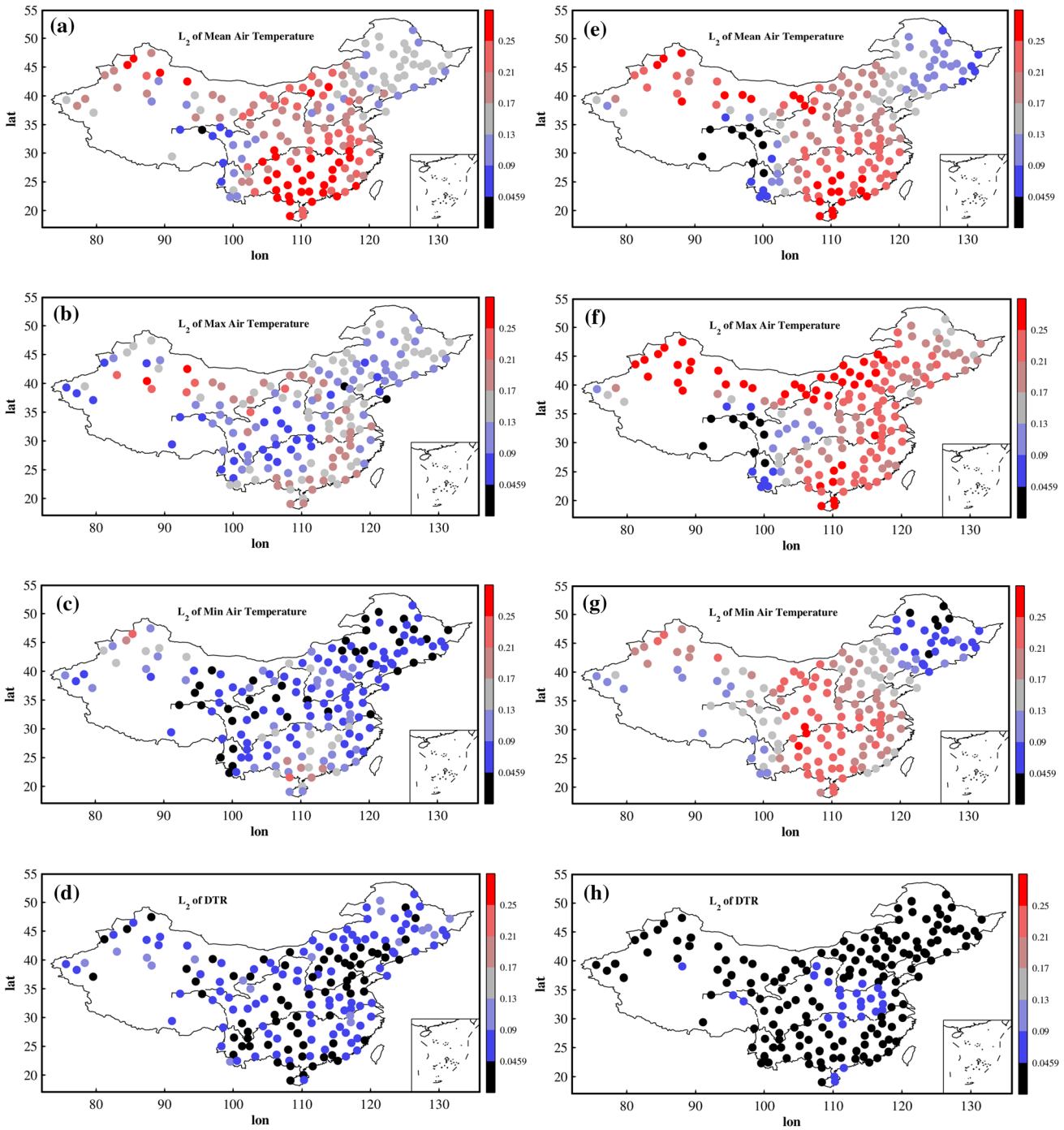

Fig. 7 L_2 to **a** T_{mean}, **b** T_{max}, **c** T_{min}, **d** DTR from 1979 to 2016 for station observations (left column) and **e** T_{mean}, **f** T_{max}, **g** T_{min}, **h** DTR for interpolated NCEP station (right column), where 0.0459 is critical threshold of L_2 at the significance level of 95% and solid black dots indicate L_2 is below this critical threshold

From above detailed results for four temperature variables, we can make the first conclusion to their differential TA behaviors. Contrary to the marked uniformly significant TA in T_{mean}, this kind of uniformly significant TA can't be found in T_{max}, T_{min} and DTR, see Fig. 2a–d. The TA is weakened in T_{max}, further weakened in T_{min} and DTR. Detailed differences are summarized in Table 1, where the mean value of L_2 over China for T_{mean} is 0.19, T_{max} is 0.14, T_{min} is 0.074, DTR is 0.056. The mean value of L_2 for DTR is close to the critical value L_{2c}.

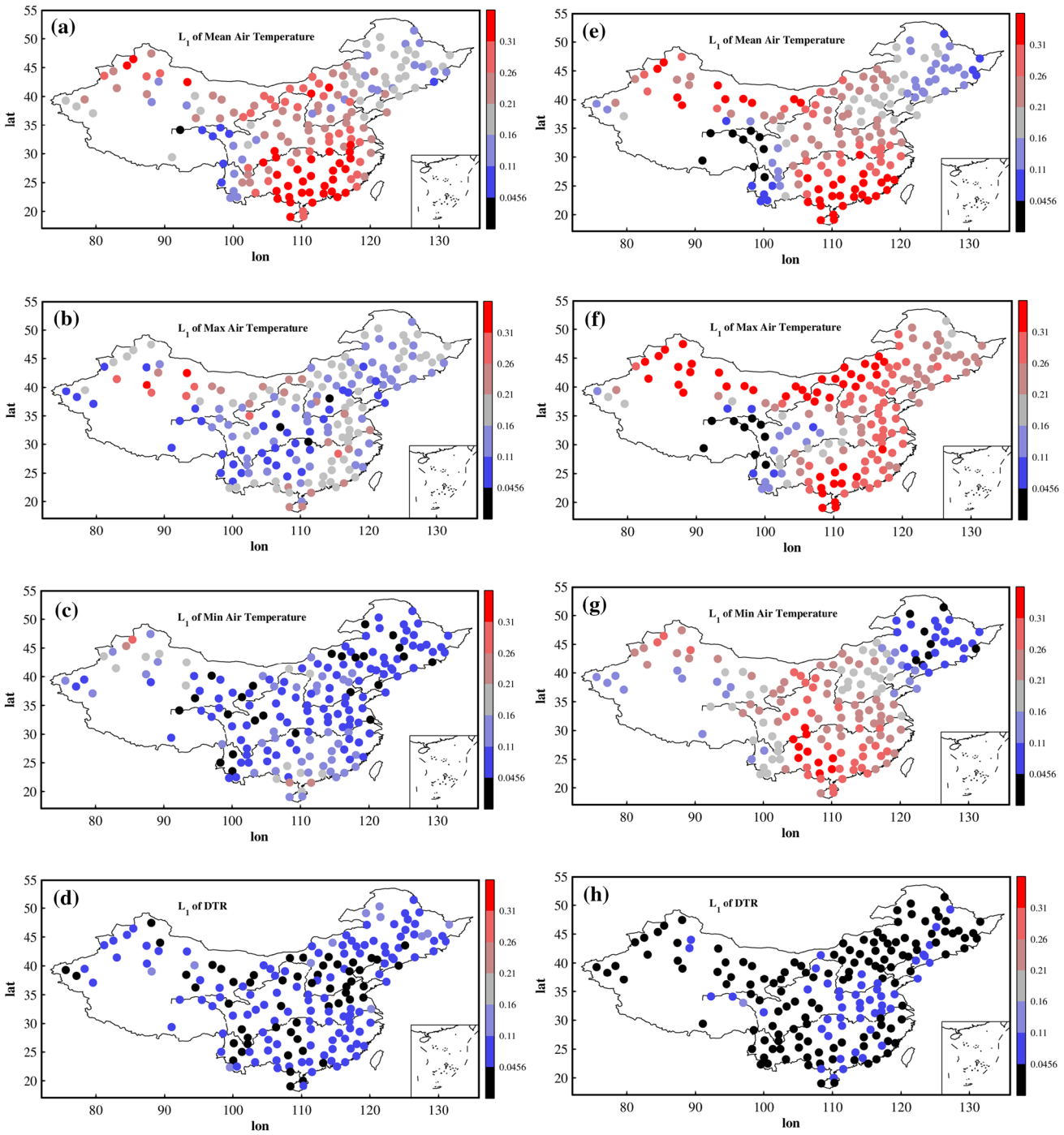

Fig. 8 L_1 to **a** T_{mean}, **b** T_{max}, **c** T_{min}, **d** DTR from 1979 to 2016 for station observations (left column) and **e** T_{mean}, **f** T_{max}, **g** T_{min}, **h** DTR for interpolated NCEP station (right column), where 0.0456 is critical threshold of L_1 at the significance level of 95% and solid black dots indicate L_1 is below this critical threshold

This distinct TA strength found in different temperature variables indicates that there are distinct temporal structures in variations of different temperature variables and correspondingly there are different factors controlling their nonlinear variations.

4.2 Consistent TA between L_2 and L_1 for four temperature variables

Previous study found that both L_2 and L_1 can reach consistent TI or TA in both outputs of theoretical asymmetry model and daily T_{mean} variations over China (Xie et al. 2016). Will

Table 1 National scale averaged L_1 and L_2 for T_{mean}, T_{max}, T_{min} and DTR from 1960 to 2016 for station observations

Data	Mean of L_2	Standard deviation of L_2	Mean of L_1	Standard deviation of L_1
T_{mean}	0.19	0.062	0.24	0.079
T_{max}	0.14	0.045	0.16	0.060
T_{min}	0.074	0.042	0.087	0.049
DTR	0.056	0.023	0.063	0.030

Table 2 National scale averaged L_1 and L_2 for T_{mean}, T_{max}, T_{min} and DTR from 1979 to 2016 for station observations

Data	Mean of L_2	Standard deviation of L_2	Mean of L_1	Standard deviation of L_1
T_{mean}	0.19	0.062	0.24	0.079
T_{max}	0.13	0.045	0.16	0.058
T_{min}	0.079	0.042	0.092	0.049
DTR	0.056	0.021	0.062	0.028

this TA consistence between L_2 and L_1 be recovered in other temperature variables' fluctuations or only specific to T_{mean}? The answer to this question is shown in Figs. 3 and 4. Figure 3 shows the spatial distribution of TA measure L_1 of four daily surface temperature variables' (including T_{mean}, T_{max}, T_{min} and DTR) observed records. Interestingly, Fig. 3 is just a perfect copy of Fig. 2 for each temperature variable if the TA measure absolute magnitude is not taken into account. There are almost the same spatial patterns for each temperature variable for both L_2 and L_1. And this perfect one to one correspondence between L_2 and L_1 can be directly observed in scatter plot of L_2 vs. L_1, see Fig. 4. For each temperature variable, L_2 and L_1 are all located in a straight line. At the same time, we can find in Fig. 4 that there are marked differential TA behaviors among these four analyzed temperature fluctuations by means of the TA strength. Actually, this well TA consistence between L_2 and L_1 can also be revealed for each temperature variables' fluctuations in the NCEP reanalysis.

From the definition of L_2 and L_1, we can see that they reflect different aspects of temporal patterns in time series. The TA consistence between L_2 and L_1 indicates they can provide the same quantitative measure to nonlinearity hidden in the analyzed time series. The mechanism resulting in this well TA consistence deserves further studies.

4.3 Length effect on TA

For all statistical analysis, the finite length effect can't be omitted. In this subsection, we will discuss what will finite size of analyzed time series affect the estimated TA measure, both L_1 and L_2. The detailed results are shown in Fig. 5, and comparative results can also be reached by comparing the results given in Figs. 2 and 3 with what have been shown in Figs. 7a–d and 8a–d. The span for analyzed temperature fluctuations in both Figs. 2 and 3 is from 1960 to 2016, but changed to from 1979 to 2016 in both Figs. 7a–d and 8a–d. The reason why we chosen the span from 1979 to 2016 in both Figs. 7a–d and 8a–d is that the span for all four temperature variables given in NCEP reanalysis is available from 1979 to 2016. Only when the finite length effect on both L_1 and L_2 is negligible, the results obtained in former sections can be compared with those from NCEP reanalysis.

For a clear-cut comparison, Fig. 5a only presents the results for T_{mean} and Fig. 5b presents the results for T_{max}, T_{min} and DTR. Obviously, both L_1 and L_2 are uniformly along the 1:1 line, which indicates that both L_1 and L_2 from 1960 to 2016 is nearly the same as those from 1979 to 2016. Finite size of under analyzed time series affects very little the estimation of both L_1 and L_2, and the correlation coefficient over two periods for L_1 is 0.984 and L_2 0.987, respectively. Similar results can be found for other three temperature variables, and all these results indicate that the results are robust to the span choice.

These results are further confirmed in the spatial distributions of both L_1 and L_2 over two different spans, see Figs. 2, 3, 7a–d and 8a–d. Both Figs. 2 and 7a–d reach nearly the same spatial patterns, and the same results are for both Figs. 3 and 8a–d. The consistent results from two different time spans are summarized in Tables 1 and 2. The National scale averaged L_1 and L_2 for four temperature variables reach nearly the same results over two time spans. There are amazing results for T_{mean}, both the mean value and standard deviation of L_1 and L_2 are equal over both spans. The results for T_{max} are also perfect, only the standard deviation of L_1 is different, with 0.60 for span from 1960 to 2016 and 0.58 for span from 1979 to 2016.

For T_{min}, the standard deviation of L_1 and L_2 are equal over both spans, there are minor different mean values for L_1 and L_2. For L_2, the mean value is 0.074 over span from 1960 to 2016 and 0.079 for span from 1979 to 2016. For L_1, the mean value is 0.087 over span from 1960 to 2016 and 0.092 for span from 1979 to 2016. While for DTR, there are negligible differences in both the mean value and the standard deviation of L_1 and L_2 over two time spans. The mean value of L_2 is equal over two spans with different standard deviation 0.023 and 0.021. While the mean value of L_1 is 0.063 with the standard deviation 0.030 over span from 1960 to 2016, and the mean value of L_1 is 0.062 with the standard deviation 0.028 over span from 1979 to 2016.

4.4 Region dependent TA

Apart from distinct TA strength found in different temperature variables, strength of TA for each temperature variable is spatially non-uniform.

For T_{mean}, both L_1 and L_2 show that the strongest TA occurs over southeast (especially over south to middle and lower reaches of Yangze River) and parts of northwest of China, see Figs. 2a and 3a. Lower TI is found in the northeast of China and Basin of Sichuan and Yun-Gui Plateau. Although different measures is applied to quantify the strength of TA in T_{mean}, this spatial patterns of TA matches well the results given in Ref. (Ashkenazy et al. 2008), where NCEP reanalysis T_{mean} was used to study rapid cooling and gradual warming at the mid-latitudes. It should be pointed out that there are predominantly zonal inhomogeneous TA patterns, zonal averaged TA will weaken its strength. At the same latitude, we can see that there is contrasting TA strength over parts of northwest of China and the northeast of China. And more significant differences are located Basin of Sichuan and Yun-Gui Plateau with weaker TA and South of China with the strongest TA.

These zonal inhomogeneous TA patterns are even more noticeable in T_{max}. For T_{max} (Figs. 2b, 3b), the higher TA mainly locates in south coastal regions, south Xinjiang and the lower reaches of Yangze River, lower TA around the upper and middle reaches of Yangze River, Basin of Sichuan and Yun-Gui Plateau. The contrasting TA patterns over different reaches of Yangze River (higher over the lower reaches and lower over reaches of Yangze River) deserve further studies.

For T_{min} (Figs. 2c, 3c), higher TA is only noticeable over northwest of Xinjiang and Guangdong province. The TA below the critical threshold can be found mainly over northeast of China, regions between Yangze River and Yellow River, and Yun-Gui Plateau. Since all TA is lower for DTR (Figs. 2d, 3d), TA below the critical threshold can be found over middle of China, which covers nearly one-third part of China. However, we can still find that the strength of TA is high over east part of northeast of China and lower reaches of Yangze River, see Figs. 2d and 3d.

4.5 Distinguishable TA between observations and reanalysis

There are TA or TI studies reported on daily mean temperature from both NCEP reanalysis (Ashkenazy et al. 2008) and observations (Bartos and Jánosi, 2005; Gyure et al. 2007; Xie et al. 2016), however, no comparison studies of TA or TI between observations and reanalysis have been carried out. At the same time, quality of reanalysis data has been evaluated from different aspects, such as long-range correlation (Zhao et al. 2017; He and Zhao 2018), however, assessment of reanalysis based on nonlinear features has not been reported. Comparison studies of TA among different temperature variables will be shown in this subsection. In order to make direct comparison between observations and reanalysis for these four temperature variables, all gridded temperature NCEP R-2 reanalysis were interpolated to the data points of measurements over each station, then we can make point-to-point comparison for each TA measure over all stations. Actually, interpolating will not change the spatial distribution and magnitude information of calculated TA measures (Figures not shown here), and this process only makes the comparison studies easier and clearer.

From above subsections, we know that the strength of TA in observations is highest in T_{mean}, followed by T_{max} and T_{min}, and the last is DTR, see Figs. 4 and 6a and Tables 1 and 2. However, for NCEP reanalysis, this order is changed. The TA strength in NCEP reanalysis is found highest in T_{max}, followed by T_{mean} and T_{min}, and the last is DTR, see Fig. 6b and Table 3. For NCEP reanalysis, TA in T_{mean} is overall only a little underestimated, TA in DTR is overall underestimated, however, TA in T_{max} and T_{min} is overall largely overestimated, see Fig. 6 and Table 3. This estimated TA departure in NCEP from observations is reflected in both mean value and standard deviation. The dispersion of TA in all temperature variables but DTR is enlarged, the same cases are found for the national scale mean value except for T_{mean} and DTR, whose mean value is reduced compared with those in observations. Especially, TA in T_{max} is exaggerated greatly, which makes T_{max} has the largest strength of TA.

The TA inconsistencies between observations and NCEP reanalysis are even more predominant in their spatial distributions. TA in T_{max} is larger than the critical threshold over nearly all regions except Tibetan Plateau, where unexpected insignificant TA is dominated, see Fig. 7f. Actually, TA over Tibetan Plateau is also markedly insignificant for T_{mean} and DTR, see Fig. 7e, h. Carefully check reveals that the overestimated TA in T_{max} is mainly due to the unexpected high TA in Xinjiang and north to upper reaches of Yellow River, see Figs. 7f and 8f. Different from what has been revealed in T_{max}, the overall TA in T_{mean} estimated from reanalysis is consistent with what has

Table 3 National scale averaged L_1 and L_2 for T_{mean}, T_{max}, T_{min} and DTR from 1979 to 2016 for NCEP reanalysis interpolated to observation station

Data	Mean of L_2	Standard deviation of L_2	Mean of L_1	Standard deviation of L_1
T_{mean}	0.18	0.065	0.23	0.091
T_{max}	0.20	0.064	0.25	0.083
T_{min}	0.17	0.056	0.20	0.077
DTR	0.045	0.017	0.055	0.020

been derived from observations. And compared to those from observations, the overall overestimated TA in T_{min} from NCEP reanalysis comes mainly from the overestimation of TA over middle of China, see Figs. 7g and 8g. For DTR, no significant larger difference in TA can be found between observations and NCEP reanalysis (see Figs. 7h, 8h). Comparing the spatial distribution of significant TA inconsistencies between observation and NCEP reanalysis, we can find the dominated regions for T_{mean}, T_{max} and T_{min} are also different. The overestimated or underestimated TA can be revealed clearly in the plot from TA measures between observation and NCEP, see Figs. 9 and 10. The consistence for T_{mean} is the best with spatial Pearson correlation coefficients 0.788 and 0.788 for L_1 and L_2, respectively, see Figs. 9a and 10a. However, the consistence for T_{min} is the worst with spatial Pearson correlation coefficients 0.432 and 0.496 for L_1 and L_2, respectively, see Figs. 9c and 10c, where TA from all stations is almost overestimated. Nearly two-thirds of TA measures for T_{max} from NCEP are overestimated (see Figs. 9b, 10b). Since all estimated TA in DTR from both observations and NCEP reanalysis are lower, the inconsistence between them is not so significant, with underestimation only over some stations, see Figs. 9d and 10d.

At last, we should point out that the consistent TA between L_2 and L_1 for four temperature variables has been revealed in observations. This good consistence is also presented in TA measure in NCEP reanalysis, see Fig. 6b. The well correspondence between L_2 and L_1 is even better in the NCEP results.

5 Conclusion and discussion

Actually, DHVG and CSID reflect different aspects of ordinal pattern hidden in the analyzed time series (Xie et al. 2016). For daily fluctuations of temperature variables, the asymmetry intensity is not very large, and the quantifiers from both DHVG (L_2) and CSID (L_1) reach nearly the same qualitative results. There are very well TA consistence between L_1 and L_2 in the observed and NCEP temperature fluctuations. Due to the easier calculations of L_1 than L_2, and the direct connection of L_1 to natural local trend in series, L_1 is recommended to be the first choice to quantify TA hidden in time series of daily variations of different temperature variables, T_{mean}, T_{max}, T_{min} and DTR. Since the calculations of L_1 are involved in the local variations of temperature fluctuations with certain steps (for daily temperature variations over

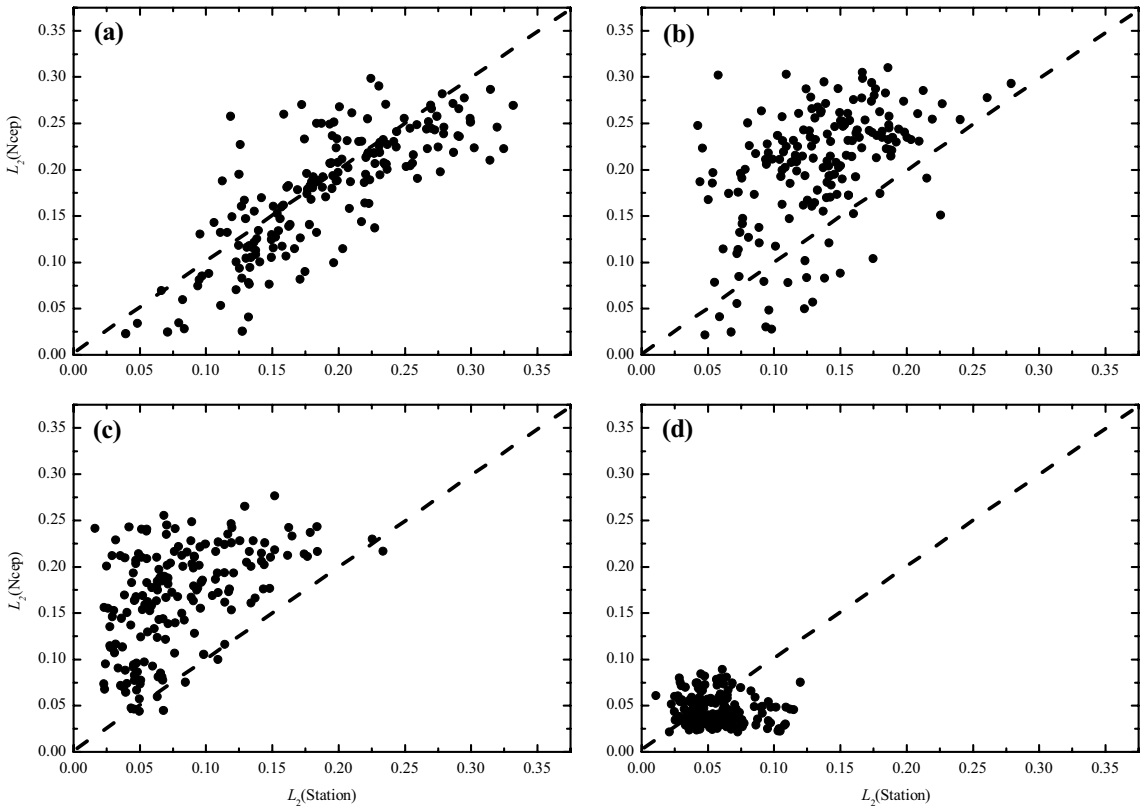

Fig. 9 L_2 scatter plots for estimations from station vs. interpolated NCEP station for T_{mean}, T_{max}, T_{min} and DTR from 1979 to 2016 for station observations. The dash black line denotes the 1:1 diagonal line

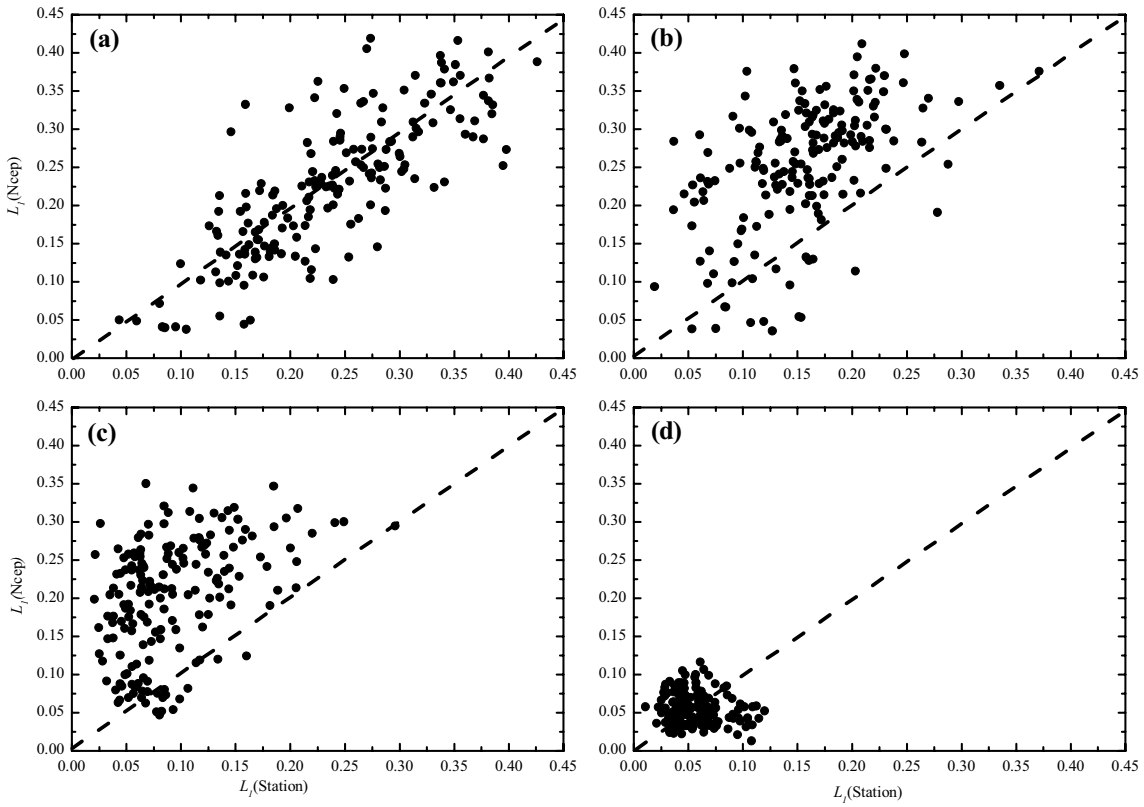

Fig. 10 L_1 scatter plots for estimations from station vs. interpolated NCEP station of T_{mean}, T_{max}, T_{min} and DTR from 1979 to 2016 for station observations. The dash black line denotes the 1:1 diagonal line

China, the maximum steps are close to 15), more detailed temporal structures of TA can be revealed compared with those from methods adopted in previous studies (Ashkenazy et al. 2008, 2016).

At the same time, distinct TA behaviors are uncovered in different temperature variables. The strength of TA from observations is highest in T_{mean} (around 0.19) and lowest in DTR (around 0.056). The strengths of TA for T_{max} (around 0.13 from observations) are overall higher than those for T_{min} (0.076 from observations). These findings are interesting, since previous studies found there are asymmetric trends in daily T_{max} and T_{min} due to different causal mechanisms in daily T_{max} and T_{min} (Karl et al 1991, 1993; Weber et al. 1994; Balling et al. 1999; Lauritsen and Rogers 2012). Different from this trend asymmetry with stronger trends in T_{min}, the asymmetry by means of TA presents with higher TA in T_{max}. And previous studies also show there are different persistent features in T_{mean}, T_{max}, T_{min} and DTR (Yuan et al. 2010; Pattanyus et al. 2004), where the long-range memory strength of T_{min} is overall a little bit higher than those for others. Both linear trend and persistence are linear characteristics of temperature variations. The new findings reported in this article are related to nonlinear features, and remarkable TA differences among T_{mean}, T_{max}, T_{min} and DTR have not been reported in the literature. Apart from distinguishable linear behavior in T_{mean}, T_{max}, T_{min} and DTR, there may be more nonlinear differential structures have not been uncovered among T_{mean}, T_{max}, T_{min} and DTR. For example, we can learn from these new findings that different natural trends in the T_{mean} may occur with unequal frequency and there are dominated natural trend patterns, however, natural trends in the DTR are symmetric and no dominated trend in its variations. These new findings may be also helpful to deep understanding the predictability in these four temperature variables' variations, since previous studies show that increasing nonlinearity can contribute to enhanced predictability in ENSO and Lorenz systems (Ye and Hsieh 2008). It was found that rapid cooling and gradual warming resulting in asymmetry in daily T_{mean} over mid-latitudes, which was conjectured to be partially related to cold fronts (Ashkenazy et al. 2008). Distinct TA structures in fluctuations of different temperature variables indicate that correspondingly there are different dominated factors controlling their nonlinear variations. It has reported that the behavior (linear or nonlinear) of T_{mean} can be free from those of T_{max} or T_{min} or DTR, and the asymmetry phenomenon in daily temperature cycle are governed by difference factors (Wang et al. 2017), such as increasing thermal storage from manmade structures,

which contributes greatly to small-scale asymmetry phenomenon in daily temperature cycle by differential impacts on T_{max} and T_{min} (Wang et al. 2017). Different TA features in four temperature variables due to different dominated factors controlling their nonlinear variations are also reflected in the fact that TA of different temperature variables' fluctuations is region-dependent. The strength of TA for each temperature variable is spatially non-uniform and it may depend on local weather or climate conditions. Therefore, the strength of TA is variable-dependent and process-dependent, and the correct simulation of this process by taking nonlinearity into account is of great importance to understand the nature of time irreversibility or temporal asymmetry.

In the previous studies, fluctuations of many atmospheric variables were often considered to be well modeled by linear processes or models, such as autoregressive (AR) processes (Storch and Zwiers 1999). It has been taken as a consensus in the literature that higher frequency daily surface temperature fluctuations can be well modeled without taking any nonlinear effect into account after proper detrending (Bartos and Janosi 2005). The findings in the study show that there are distinguished TA strength differences among different temperature variables' variability, so this consensus may be not universally applied to these temperature variables' variability. In order to reproduce these differential TA features, nonlinear effects should be differentially included in the newly rebuilt models.

Distinguishable TA features between observations and reanalysis provides a novel index to evaluate the quality of reanalysis (Zhao et al. 2017; He and Zhao 2018) from the nonlinear point of view. This is of great importance in extreme event related studies and understanding to small-scale phenomenon, since the nonlinearity is closely related to extreme events and certain small-scale phenomena (Raghavendra et al. 2018). There are significant estimated TA differences between observations and reanalysis over some specific regions for specific temperature variable, such as T_{mean} in Southern parts of East China, T_{max} in Northwest China and Western Inner Mongolia and T_{min} over middle of China. The quality of NCEP reanalysis is questionable over these regions for some specific temperature variables. Contrary to the results based on long-range correlation, where the quality of NCEP reanalysis T_{max} is best among four temperature variables (Zhao et al. 2017; He and Zhao 2018), the worst quality of NCEP reanalysis is revealed in T_{min} and T_{max} based on nonlinear measures (i.e., TA). This indicates the assessment of NCEP reanalysis from linear feature may be different from those from nonlinear feature. At the same time, due to rare observations over Tibetan Plateau, where TA calculated from NCEP reanalysis for all temperature variables is different from those estimated from observations. Although the results of TA for all temperature variables over these regions require further check, the conclusions are consistent with what has been reached based on long-term correlation (He and Zhao 2018). The quality of reanalysis over these regions is questionable, since the problem how to correctly model the terrain of Tibetan Plateau is still unsolved in all related studies (He and Zhao 2018). True physical processes not completely including in related models may lead to distorted modeling or missing important structure information, and if outputs of these models are assimilated into reanalysis, they can cause distinguishable features between observations and reanalysis, such as bias in the variance of gridded data sets can lead to misleading conclusions about changes in climate variability and extremes (Begueria et al. 2016). And it has been reported that compared to the well modeled daily mean temperature, there are larger variability and inconsistency between observed and modeled daily minimum temperature and maximum temperature, where the daily minimum temperature is overestimated and the daily maximum temperature is underestimated (Raghavendra et al. 2018). So the modeled daily minimum temperature and maximum temperature are considered not suitable to study the extreme events, such as heat-waves (Raghavendra et al. 2018). The marked mismatch between observations and reanalysis found in this paper also indicates that the nonlinear conclusions or extreme event studies related to T_{max}, T_{min} and DTR reanalysis should be reevaluated and it is also of great important to reevaluate the performance of certain models over China, such as outputs from CMIP5 models (He et al. 2018).

Distinct TA behaviors in different temperature variables, region-dependent TA behaviors and distinguishable TA features between observations and reanalysis indicate that there are still many works required to understand the true dominated factors controlling the variations of specific temperature variables. One of urgently unsolved problems is what has caused the marked TA and why there are distinct TA behaviors in different temperature variables. If this problem is solved, it will contribute greatly to the understanding of region-dependent TA behaviors and distinguishable TA features between observations and reanalysis. There are some clues on solving this problem, such as cold fronts (Ashkenazy et al. 2008) for rapid cooling and gradual warming asymmetry in daily T_{mean} over mid-latitudes. However, temperature TA mechanism studies remain deficient compared with the in-depth studies on asymmetry of ENSO, where it has been found that warm-cold magnitude asymmetry is closely related to nonlinear advection heating (An and Jin 2004; An 2004; Su et al. 2010), the specific mechanisms over different phases for asymmetry of ENSO are also different, and they may be related different mean states (An and Jin 2004; An 2004; Ye and Hsieh 2006; Su et al. 2010; Choi et al. 2012). Mechanisms causing TA in temperature fluctuations can draw lessons from these in-depth studies.

Acknowledgements The authors thank the editor and reviewers for their valuable comments and suggestions on improving our presentation. This research was supported by the National Natural Science Foundation of China through Grants (Nos. 41475048 and 41705041).

References

An SI (2004) Interdecadal changes in the El Nino-La Nina asymmetry. Geophys Res Lett 31:L23210

An SI, Jin FF (2004) Nonlinear and asymmetry of ENSO. J Clim 17:2399–2412

Ashkenazy Y, Tziperman E (2004) Are the 41 kyr glacial oscillations a linear response to Milankovitch forcing? Quat Sci Rev 23:1879–1890

Ashkenazy Y, Feliks Y, Gildor H, Tziperman E (2008) Asymmetry of daily temperature records. J Atmos Sci 65:3327

Ashkenazy Y, Fredj E et al (2016) Current temporal asymmetry and the role of tides: Nan-Wan bay vs. the gulf of Elat. Ocean Sci 12:733

Balling RC, Periconi DA, Corveny RS (1999) Large asymmetric temperature trends at Mount Wilson, California. Geophys Res Lett 26:2753

Bartos I, Janosi IM (2005) Atmospheric response function over land: strong asymmetries in daily temperature fluctuations. Geophys Res Lett 32:L23820

Begueria S, Vicente-Serrano SM, Tomas-Burgueraa M, Manetac M (2016) Bias in the variance of gridded data sets leads to misleading conclusions about changes in climate variability. Int J Climatol 36:3413–3422

Bisgaard S, Kulahci M (2011) Time series analysis and forecasting by example. Wiley, New York

Bunde A, Eichner JF, Kantelhardt JW, Havlin S (2005) Long-term memory: a natural mechanism for the clustering of extreme events and anomalous residual times in climate records. Phys Rev Lett 94:048701

Burykin A, Costa M, Peng CK, Goldberger AL, Buchman TG (2011) Generating signals with multiscale time irreversibility: the asymmetric weierstrass function. Complexity 16:29

Cammarota C, Rogora E (2006) Time reversal, symbolic series and irreversibility of human heartbeat. Chaos Solitons Fractals 32:1649–1654

Choi J, An SI, Yeh SW (2012) Decadal amplitude modulation of two types of ENSO and its relationship with the mean state. Clim Dyn 38:2631–2644

Costa M, Goldberger AL, Peng CK (2005) Broken asymmetry of the human heartbeat: loss of time irreversibility in aging and disease. Phys Rev Lett 95:198102

Costa M, Peng CK, Goldberger AL (2008) Multiscale analysis of heart rate dynamics: entropy and time irreversibility measures. Cardiovasc Eng. https://doi.org/10.1007/s10558-007-9049-1

Cover TM, Thomas JA (2006) Elements of information theory. Wiley, Hoboken

Daw CS, Finney CEA, Kennel MB (2000) Symbolic approach for measuring temporal irrevetsibility. Phys Rev E 62:1912–1921

Deng QM, Nian D, Fu ZT (2018) The impact of inter-annual variability of annual cycle on long-term persistence of surface air temperature in long historical records. Clim Dyn 50:1091–1100

Diks C, van Houwelingen JC, Takens F, DeGoede J (1995) Reversibility as a criterion for discriminating time series. Phys Lett A 201:221–228

Ding RQ, Li JP, Tseng YH (2015) The impact of South Pacific extratropical forcing on ENSO and comparisons with the North Pacific. Clim Dyn 44:2017–2034

Ding RQ, Li JP, Zheng F, Feng J, Liu DQ (2016) Estimating the limit of decadal-scale climate predictability using observational data. Clim Dyn 46:1563–1580

Donges JF, Donner RV, Kurths J (2013) Testing time series irreversibility using complex network methods. EPL 102:10004

Donner RV, Zou Y, Donges JF, Marwan N, Kurths J (2010) Recurrence networks: a novel paradigm for nonlinear time series analysis. New J Phys 12:033025

Douglass DH (2010) El Nino-Southern Oscillation: magnitudes and asymmetry. J Geophys Res 115:D15111

Eichner JF, Kantelhardt JW, Bunde A, Havlin S (2007) Statistics of return intervals in long-term correlated records. Phys Rev E 75:011128

Fu ZT, Shi L, Xie FH, Piao L (2016) Nonlinear features of Northern annular mode variability. Phys A 449:390

Gao M, Franzke CLE (2017) Quantile regression-based spatiotemporal analysis of extreme temperature change in China. J Clim 30:9897

Govindan RB, Wilson JD, Preiβl H, Eswaran H, Campbell JQ, Lowery CL (2007) Detrended fluctuation analysis of short datasets: an application to fetal cardiac data. Phys D 226:23

Gyure B, Bartos I, Janosi IM (2007) Nonlinear statistics of daily temperature fluctuations reproduced in a laboratory experiment. Phys Rev E 76:037301

He WP, Zhao SS (2018) Assessment of the quality of NCEP-2 and CFSR reanalysis daily temperature in China based on long-range correlation. Clim Dyn 50:493

He WP, Zhao SS, Wu Q, Jiang YD, Wan SQ (2018) Simulating evaluation and projection of the climate zones over China by CMIP5 models. Clim Dyn. https://doi.org/10.1007/s00382-018-4410-1

Heinrich H (2004) Origin and consequences of cyclic ice rafting in the Northeast Atlantic Ocean during the past 130,000 years. Quat Res 29:142–152

Hou ZL, Li JP, Ding RQ, Feng J, Duan WS (2017) The application of nonlinear local Lyapunov vectors to the Zebiak–Cane model and their performance in ensemble prediction. Clim Dyn 51:283–304

Hoyt DV, Schatten KH (1998a) Group sunspot numbers: a new solar activity reconstruction. Part 1. Solar Phys 179:189–219

Hoyt DV, Schatten KH (1998b) Group sunspot numbers: a new solar activity reconstruction. Part 2. Solar Phys 181:491–512

Hutchinson DK, England MH, Santoso A, Hogg AM (2013) Interhemispheric asymmetry in transient global warming: the role of Drake Passage. Geophys Res Lett 40:1587–1593

Kalnay E et al (1996) The NCEP/NCAR 40-year reanalysis project. Bull Am Meteorol Soc 77:437

Kanamitsu M et al (2002) NCEP-DOE AMIP-II reanalysis (R-2). Bull Am Meteorol Soc 83:1631

Karl TR, Kukla G et al (1991) Global warming: evidence for asymmetric diurnal temperature change. Geophys Res Lett 18:2253

Karl TR, Jones PD et al (1993) A new perspective on recent global warming: asymmetric trends of daily maximum and minimum temperature. Bull Am Meteorol Soc 74:1007

King T (1996) Quantifying nonlinearity and geometry in time series of climate. Quat Sci Rev 15:247–266

Kiraly A, Janosi IM (2002) Stochastic modeling of daily temperature fluctuations. Phys Rev E 65:051102

Koscielny-Bunde E, Bunde A, Havlin S, Roman HE (1998) Indication of a universal persistence law governing atmospheric variability. Phys Rev Lett 81:729

Kowalski AM, Martin MT, Plastino A, Rosso OA, Casas M (2011) Distances in probability space and the statistical complexity setup. Entropy 13:1055–1075

Lacasa L, Luque B, Ballesteros F, Luque J, Nuno JC (2008) From time series to complex networks: the visibility graph. Proc Natl Acad Sci 105:4972–4975

Lacasa L, Nunez A, Roldan E, Parrondo JMR, Luque B (2012) Time series irreversibility: a visibility graph approach. Eur Phys J B 85:217

Lauritsen RG, Rogers JC (2012) U.S. Diurnal temperature range variability and regional causal mechanisms, 1901–2002. J Clim 25:7216

Li Q, Zhang H, Chen J, Li W, Liu X, Jones P (2009) A mainland China homogenized historical temperature dataset for 1951–2004. Bull Am Meteorol Soc 90:1062

Li QL, Fu ZT, Yuan NM (2015) Beyond Benford's law: distinguishing noise from chaos. PLoS One 10:e0129161

Li JP, Feng J, Ding RQ (2018) Attractor radius and global attractor radius and their application to the quantification of predictability limits. Clim Dyn 51:2359–2374

Lisiecki LE, Raymo ME (2005) A Pliocene–Pleistocene stack of 57 globally distributed benthic delta O-18 records. Paleoceanography 20:PA1003. https://doi.org/10.1029/2004PA001071

Livina V, Ashkenazy Y, Kizner Z, Strygin V, Bunde A, Havlin S (2003) A stochastic model of river discharge fluctuations. Phys A 330:283–290

Ludescher J, Bunde A, Franzke CLE, Schellnhuber HJ (2016) Long-term persistence enhances uncertainty about anthropogenic warming of Antarctica. Clim Dyn 46:263–271

Luque B, Lacasa L, Ballesteros F, Luque J (2009) Horizontal visibility graphs: exact results for random time series. Phys Rev E 80:046103

Maddox RA, Perkey DJ, Fritsch JM (1981) Evolution of upper tropospheric features during the development of a mesoscale convective complex. J Atmos Sci 38:1664

Makse HA, Havlin S, Schwartz M, Stanley HE (1996) Method for generating long-range correlations for large systems. Phys Rev E 53:5445

Pattanyus-Abraham M, Kiraly A, Janosi IM (2004) Nonuniversal atmospheric persistence: different scaling of daily minimum and maximum temperatures. Phys Rev E 69:021110

Raghavendra A, Dai AG, Milrad SM, Cloutier-Bisbee SR (2018) Floridian heatwaves and extreme precipitation-future climate projections. Clim Dyn. https://doi.org/10.1007/s00382-018-4148-9

Roldan E, Parrondo JMR (2010) Estimating dissipation from single stationary trajectories. Phys Rev Lett 105:150607

Schreiber T, Schmitz A (1996) Improved surrogate data for nonlinearity tests. Phys Rev Lett 77:635–638

Stone L, Landan G, May RM (1996) Detecting time's arrow: a method for identifying nonlinearity and deterministic chaos in time-series data. Proc R Soc Lond B 263:1509–1513

Su JZ, Zhang RH, Li T, Rong XY, Kug JS, Hong CC (2010) Causes of the El Nino and La Nina amplitude asymmetry in the equatorial Eastern Pacific. J Clim 23:605–617

von Storch H, Zwiers FW (1999) Statistical analysis in climate research. Cambridge Univ Press, Cambridge

Wang K, Li Y, Wang Y, Yang X (2017) On the asymmetry of the urban daily air temperature cycle. J Geophys Res Atmos 122:5625–5635

Weber RO, Talkner P, Stefanicki G (1994) Asymmetric diurnal temperature change in the Alpine region. Geophys Res Lett 21:673

Weiss G (1975) Time-reversibility of linear stochastic processes. J Appl Probab 12:831–836

Xie FH, Fu ZT, Piao L, Mao JY (2016) Time irreversibility of mean temperature anomaly variations over China. Theor Appl Climatol 123:161

Yang ACC, Huseu SS, Yien HW, Goldberger AL, Peng CK (2003) Linguistic analysis of the human heartbeat using frequency and rank order statistics. Phys Rev Lett 90:108103

Ye ZQ, Hsieh WW (2006) The influence of climate regime shift on ENSO. Clim Dyn 26:823–833

Ye ZQ, Hsieh WW (2008) Enhancing predictability by increasing nonlinearity in ENSO and Lorenz systems. Nonlin Processes Geophys 15:793–801

Yuan NM, Fu ZT (2014) Century-scale intensity modulation of large-scale variability in long historical temperature records. J Clim 27:1742

Yuan NM, Fu ZT, Mao JY (2010) Different scaling behaviors in daily temperature records over China. Phys A 389:4087

Yuan NM, Fu ZT, Mao JY (2013) Different multi-fractal behaviors of diurnal temperature range over the north and the south of China. Theor Appl Climatol 112:673

Yuan NM, Huang Y, Duan JP et al (2018) On climate prediction: how much can we expect from climate memory? Clim Dyn. https://doi.org/10.1007/s00382-018-4168-5

Zhai PM, Pan XL (2003) Trends in temperature extremes during 1951–1999 in China. Geophys Res Lett 30:1913

Zhao SS, He WP, Jiang YD (2017) Evaluation of NCEP-2 and CFSR reanalysis seasonal temperature data in China using detrended fluctuation analysis. Int J Climatol. https://doi.org/10.1002/joc.5173